

Figures

Figure 5 (cover of chapter I on page 29): The ribosome during stress

During normal growth conditions there are three tRNA binding sites (A, P and E) that can be occupied whereas in the cold only one tRNA can bind to the E site. A and P site are blocked by Protein Y in the cold.

30S under normal growth conditions shown in red, under cold shock conditions in blue. Red 30S: tRNA bound to the A, P and E site are shown in cyan, yellow and blue, respectively. Blue 30S: Protein Y and E site tRNA are shown in yellow and blue, respectively.

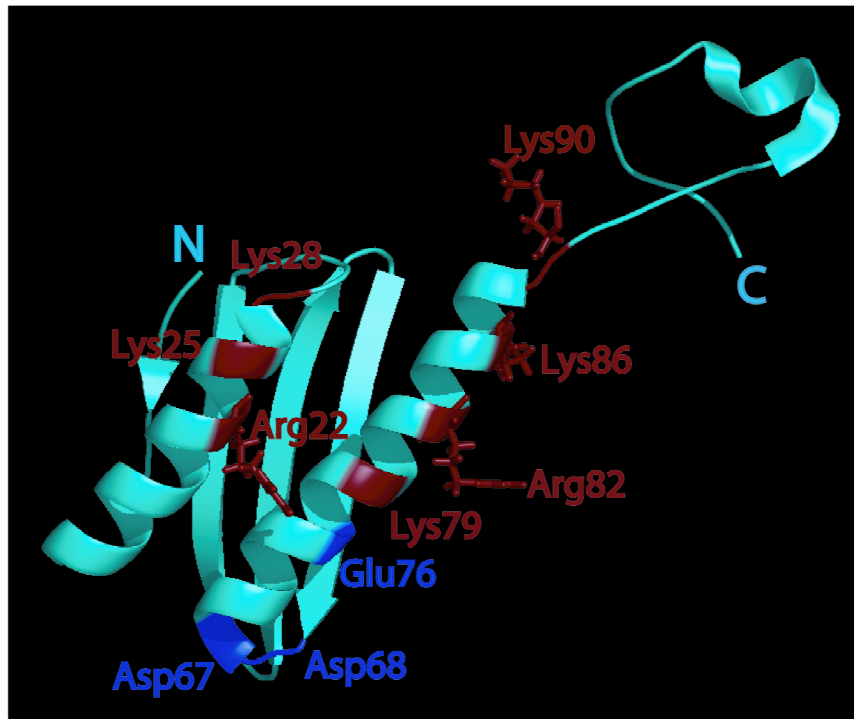
Figure 6: Sequence and structure homologues of Protein Y

A Sequence homologues of PY, which NMR structure is shown here (Ye, Serganov et al. 2002), were found in over 50 bacterial genomes as well as in plant genomes. Most of the conserved residues are located in the N-terminal part of the protein, whereas the C-terminal part is disordered. Conserved surface features include the positively charged residues located at the C-terminal part of the α -helices (Arg22, Lys25, Lys28, Lys79, Arg82, Lys86, Lys90) as well as negatively charged residues at the N-terminal part of the helices (Glu75, Glu76, Asp68).

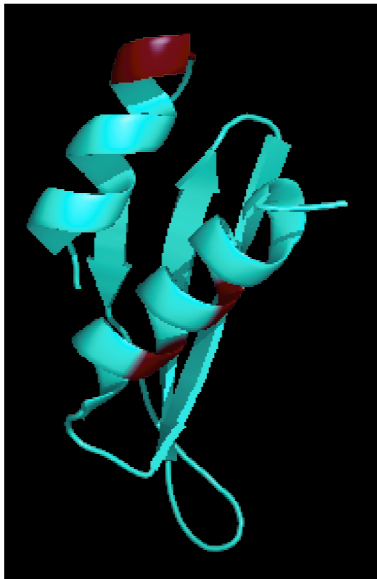
B NMR structure of the third dsRBD (double stranded RNA binding domain) of *Drosophila melanogaster* Staufen protein (Ramos, Grunert et al. 2000), a structure homolog of PY, is shown. Conserved positively charged residues located at the two α -helices of the dsRBD are shown in red.

C NMR structure of the third dsRBD of the *Drosophila* Staufen protein (Ramos, Grunert et al. 2000) show that residues within the loop region of the protein are in contact with the RNA backbone. Residues located in the second and fourth loop of the dsRBD are in contact with the minor and major groove of the RNA, respectively.

A



B



C

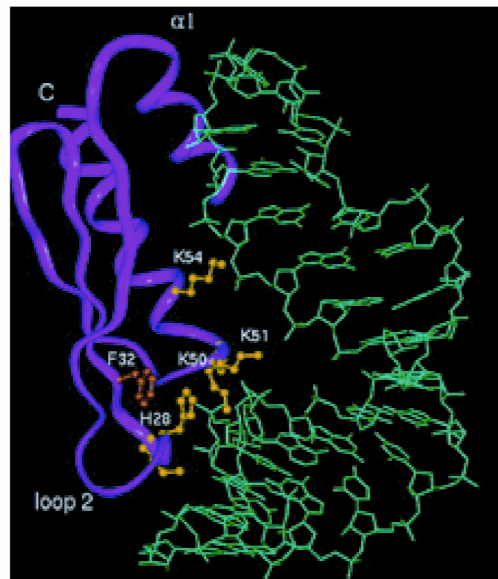


Figure 7: I422 crystals of 70S *E. coli* ribosomes

A Crystals of the 70S *E. coli* ribosome were grown using the vapor diffusion method resulting in different sizes dependent of the growth time. The ruler ranges from 0 to 500 μm .

B The crystals were grown in the exact same conditions as previously described (Vila-Sanjurjo, Ridgeway et al. 2003) and resulted in the same space group I422.

The unit cell parameters for the new crystal form, containing five ribosomes per asymmetric unit are: $a, b = 680\text{\AA}$, $c = 1900\text{\AA}$, $\alpha, \beta, \gamma = 90^\circ$ (left site). The unit cell parameters for the old crystal form that contained only one ribosome per asymmetric unit are: $a, b = 680\text{\AA}$, $c = 380\text{\AA}$, $\alpha, \beta, \gamma = 90^\circ$ (right site).

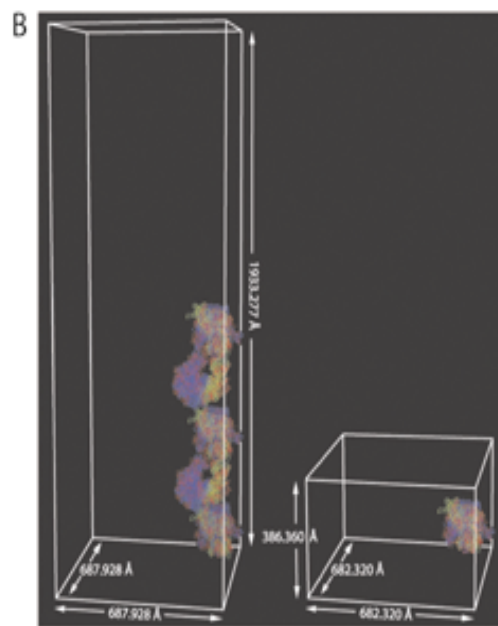
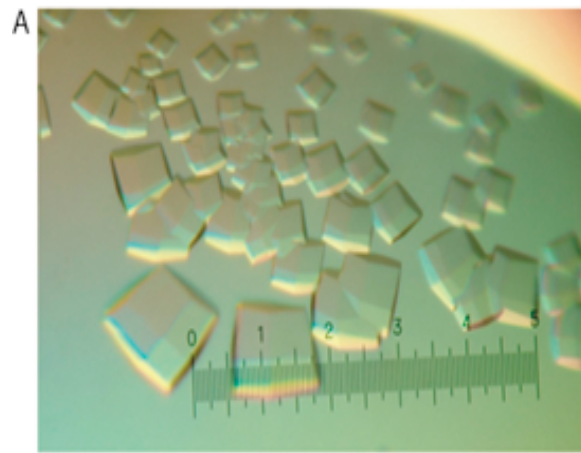


Figure 8: Ribosomes in the asymmetric unit

One asymmetric unit contained 5 copies of the ribosome that all included one copy of Protein Y. Their position to one another in the crystal packing is shown.

The large 50S subunit is shown in blue, the small 30S subunit in yellow, Protein Y is shown in red.

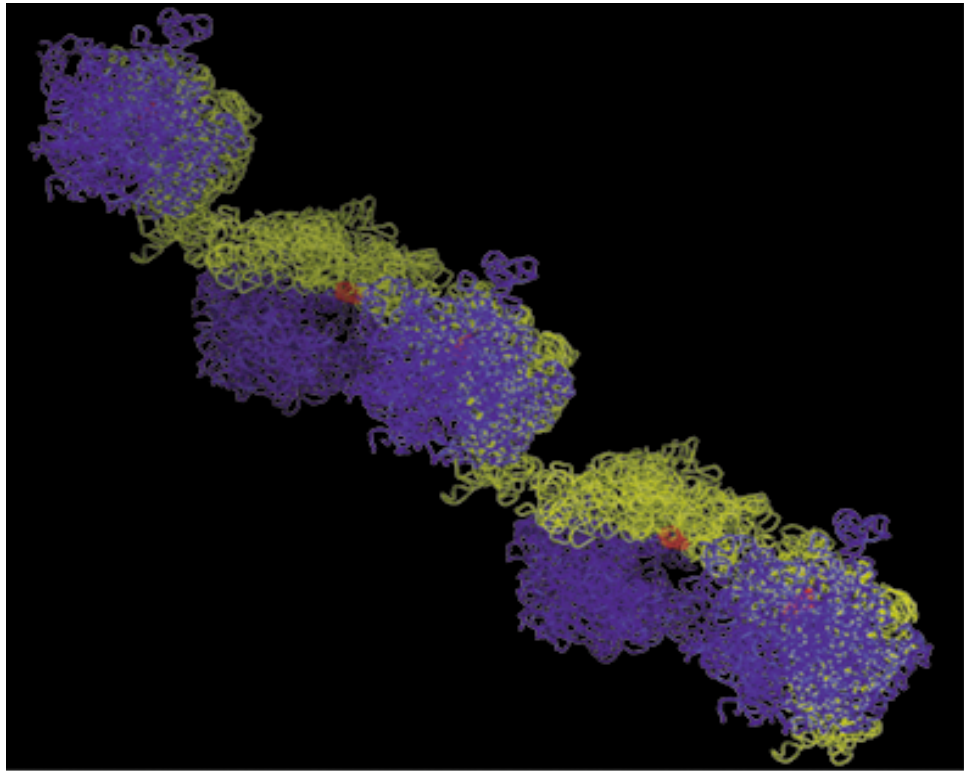
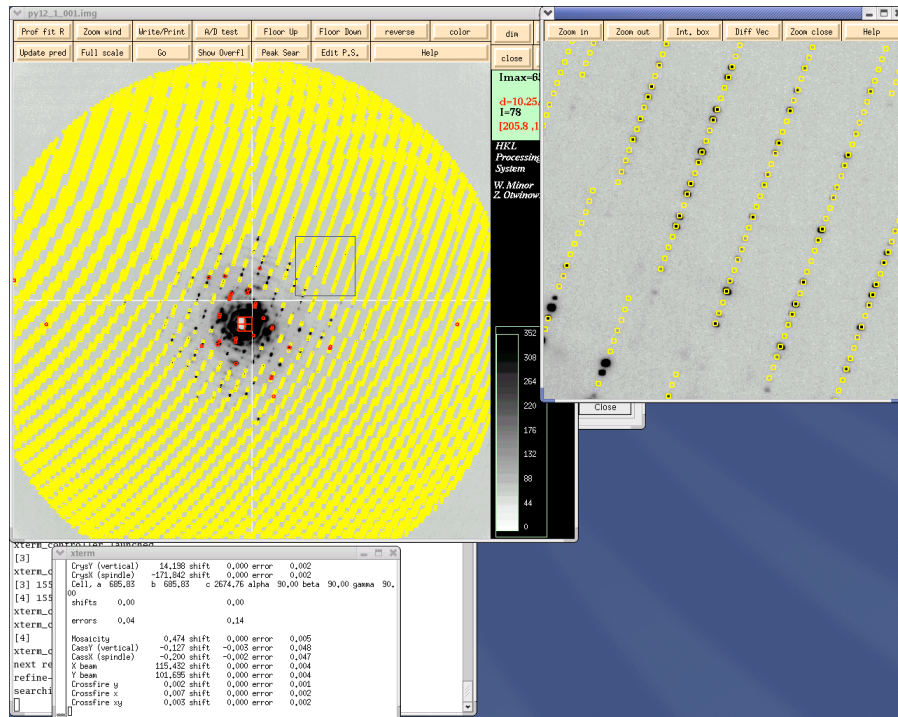


Figure 9: Indexing of diffraction patterns of the large cell

The diffraction pattern of the large cell (5 ribosomes in the asymmetric unit) indexed in

A with the parameters: $a, b = 687\text{\AA}, c = 1933\text{\AA}; \alpha, \beta, \gamma = 90^\circ$ can also be indexed as **B** the small cell (1 ribosome in the asymmetric unit) with the parameters: $a, b = 682\text{\AA}, c = 386\text{\AA}; \alpha, \beta, \gamma = 90^\circ$.

A



B

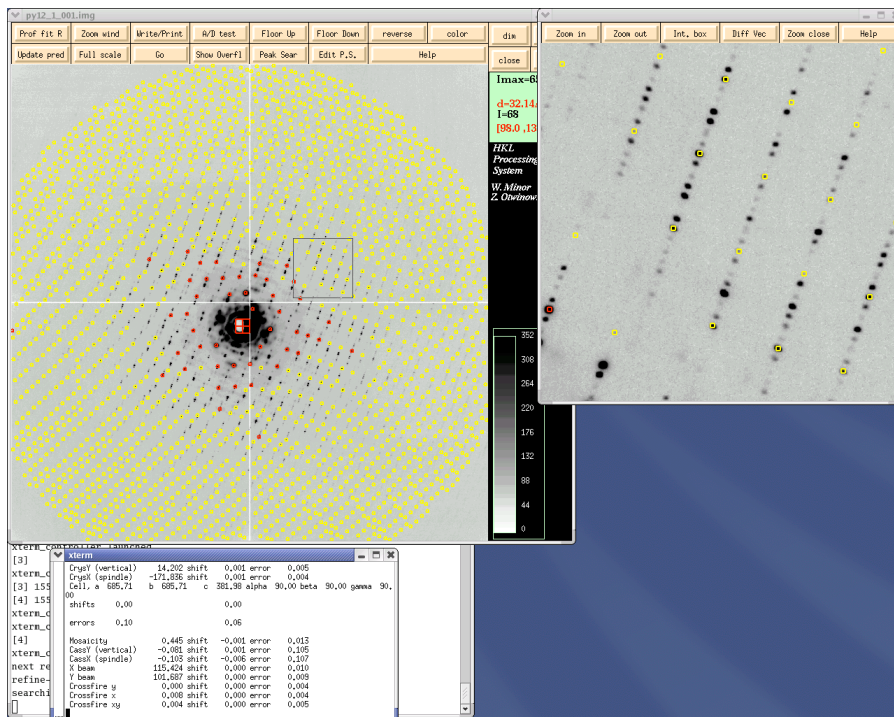
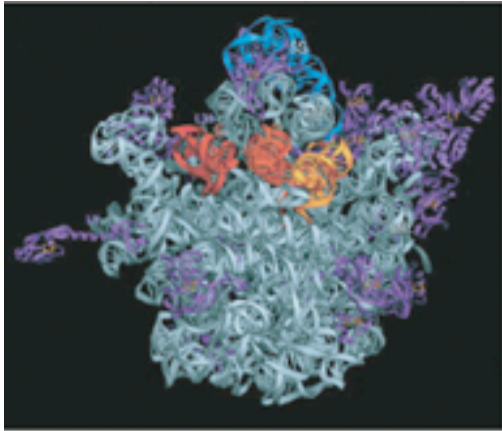
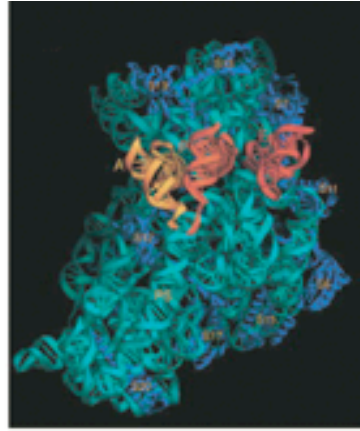


Figure 10: Molecular replacement solution

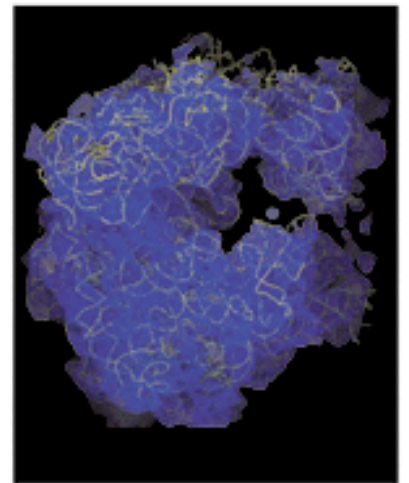
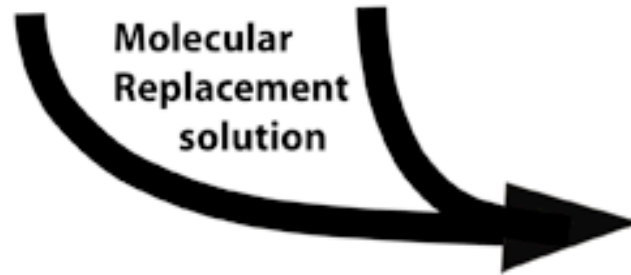
The phase problem was solved by molecular replacement. Using the atomic resolution structures of the 50S subunit from *Deinococcus marismortui* (Schluenzen, Zarivach et al. 2001) and the 30S subunit from *thermos thermophilus* (Wimberly, Brodersen et al. 2000) a model for the *E. coli* ribosome was build by molecular replacement for one ribosome. The model for the new unit cell containing five ribosomes per asymmetric unit was build by using rigid body refinement (CNS-program (Brünger, Adams et al. 1998)). The $F_{\text{obs}} - F_{\text{obs}}$ difference map of the crystals containing PY and the empty 70S crystals resulted in the postive density for PY.



Deinococcus radiodurans 50S
(Schluenzen, et al., 2001)



Thermus thermophilus 30S
(Wimberly et al, 2000)



11.4A wt E.coli structure



5 70S ribosomes / asu

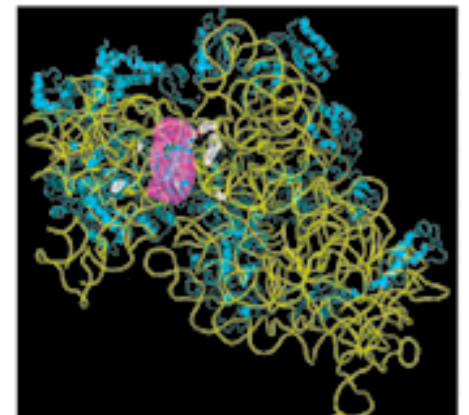
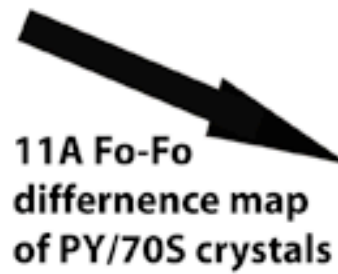


Figure 11: Structural model of Protein Y binding to the ribosome as determined by x-ray crystallography

A Location of PY's density in the 70S ribosome. The 30S subunit is shown in gold, the 50S subunit in light blue, positive difference electron density in blue, negative density in red, and PY in cyan. Helix 69 of 23S rRNA, known to be involved in the subunit association as well as signal transmission between the two subunits is marked with an asterisk (H = head region of 30S subunit; B = body region of 30S subunit; CP = central perturbation of 50S subunit). The arrow shows the perspective for **B**.

B PY density in the 30S subunit as seen from the perspective of the subunit interface, indicated by the arrow in **A**. The density occurs between the platform (P) and the head (H) of the 30S subunit; PY lies in between the A and P site of the 30S subunit. The A-, P- and E sites, and the body (B) of the small subunit are marked;

C Details of the docking of the N-terminal core of PY (accession code 1L4S (Ye, Serganov et al. 2002)) into the difference electron density. The structure did not reveal any density for the disordered C-terminal tail, its position is indicated. The view is from the perspective of the arrow in **B**.

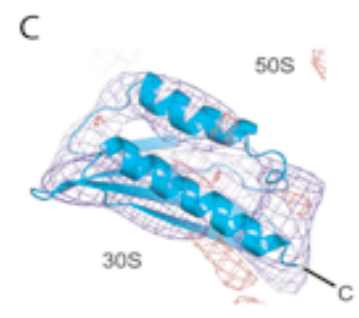
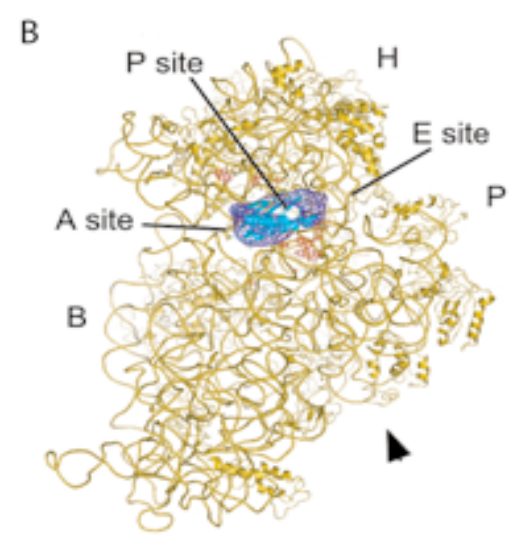
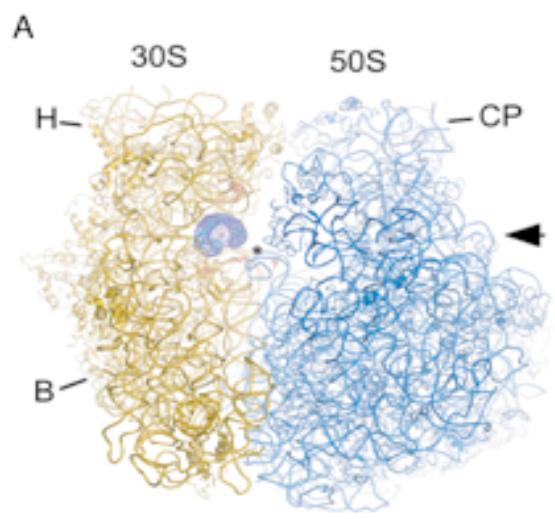


Figure 12: Detailed view on the PY binding site within the ribosome

A Superposition of A, P and E site tRNA with the structure containing PY reveal that PY's density (shown in dark blue) overlaps with the binding site of the A and P site tRNA. A-, P- and E site tRNAs (Yusupov, Yusupova et al. 2001) are colored cyan, green and grey, respectively. The positions of the 30S and 50S subunits, the path of mRNA (5' to 3'), and the location of the C-terminal tail of PY are indicated.

B Superposition of A, P and E site tRNAs (color coded as above) and mRNA (Yusupova, Yusupov et al. 2001) with the PY structure show that the protein only slightly overlaps with the binding site of the mRNA, shown here in red. The 5' and 3' ends of the mRNA are marked.

C Stereo view of the location of critical 16S rRNA residues G926, C1400, C1402 and A1493 (green) relative to PY as characterized by chemical probing. Helix 69 (H69) of 23S rRNA is shown in blue. The NMR structure of PY (cyan) (Ye, Serganov et al. 2002) was used to dock it into the electron density, shown in dark blue. Conserved residues within PY are shown in magenta (Ye, Serganov et al. 2002).

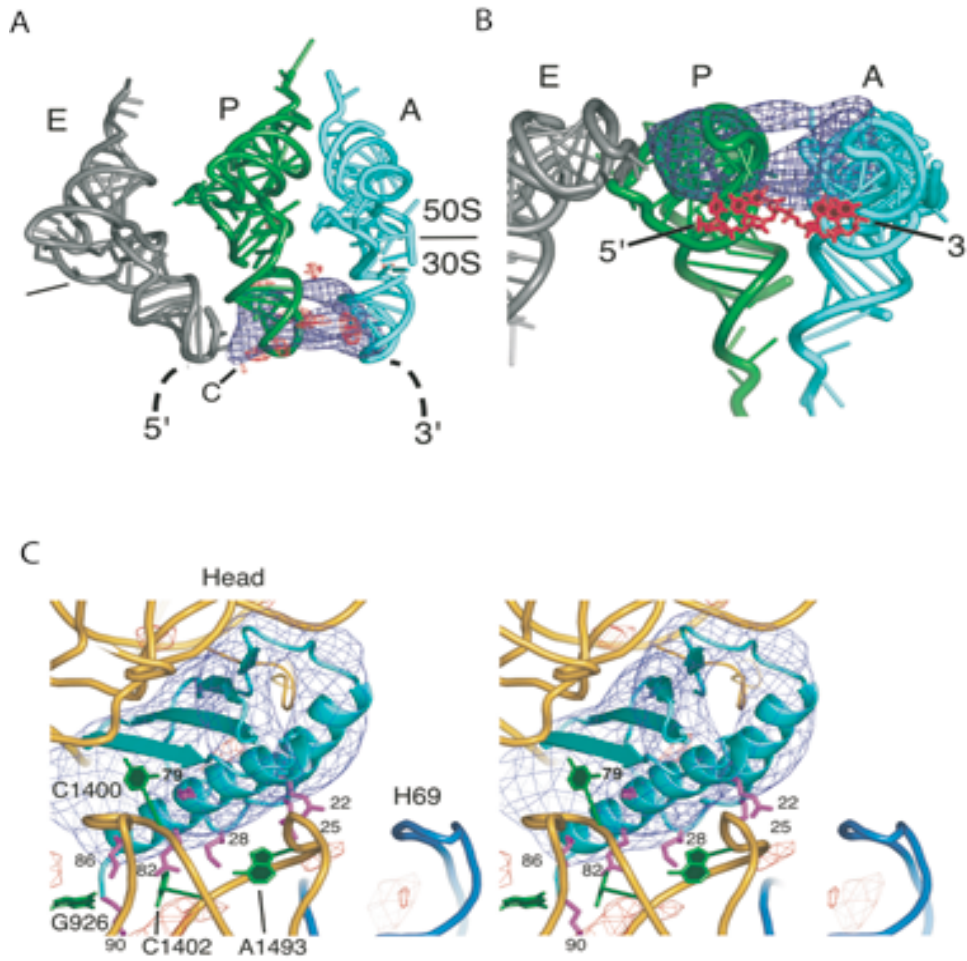


Figure 13: Chemical probing of the ribosome in the presence of PY

A DMS probing of the 16S rRNA in the region of nucleotides A1492-1493, which are characteristic sites for tRNA binding to the ribosomal A site (Moazed and Noller 1989).

B Kethoxal probing of 16S rRNA in the region of nucleotide G926, a diagnostic site for P site tRNA binding (Prince, Taylor et al. 1982), (Moazed and Noller 1989).

C Dimethyl sulfate (DMS) probing of the 16S rRNA in the region of nucleotide C1400 (Moazed and Noller 1989), (Prince, Taylor et al. 1982) and C1402 (Vila-Sanjurjo and Dahlberg 2001), again a diagnostic site for P site tRNA binding.

D DMS probing of the 23S rRNA in the region of nucleotide C2394, a critical site for tRNA binding to the E site (Moazed and Noller 1989).

Sequencing lanes are marked by A, C, G, or U. Samples are as indicated above each panel.

E Schematic view of the experiment. Protein Y was pre-incubated with the ribosomes before the addition of Poly-U mRNA and an amount of tRNA suitable to bind to all three tRNA sites. All chemical probing experiments for A, P and E site respectively were done at the same time using the same sample.

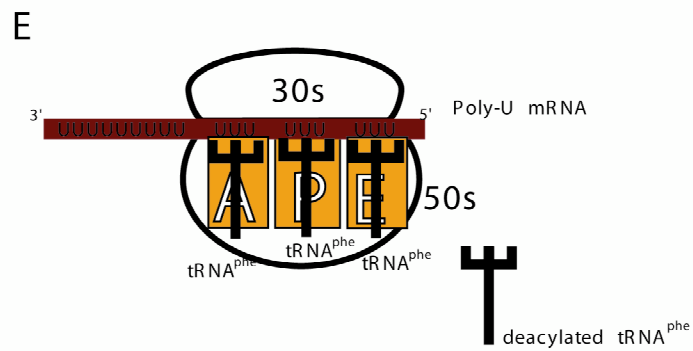
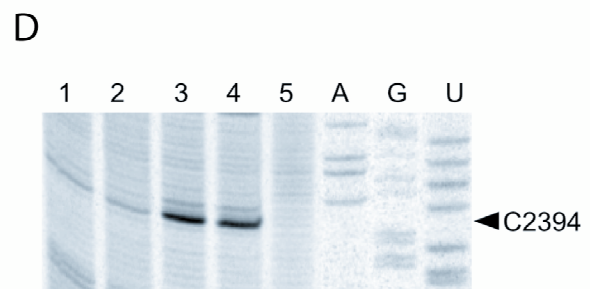
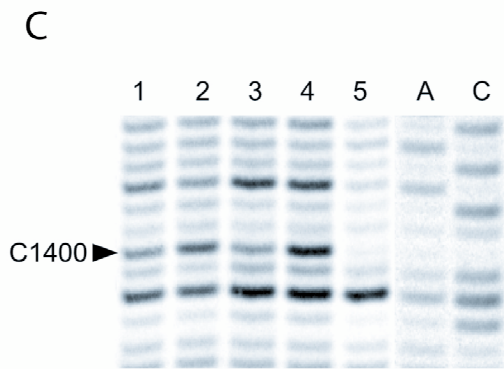
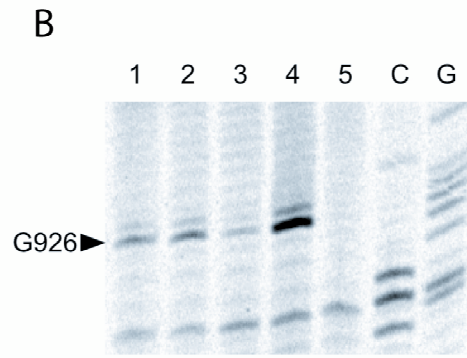
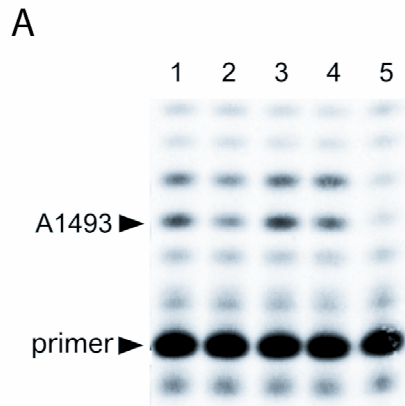


Figure 14: Inhibition of P-site tRNA binding by PY

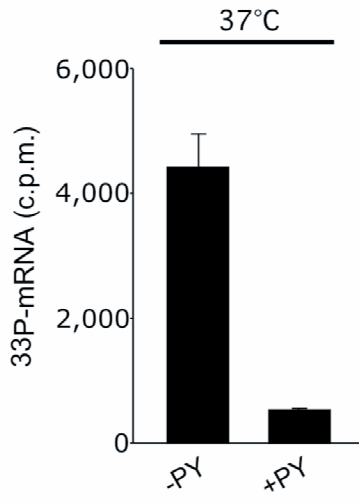
A Binding of deacylated tRNA^{fMet} to ribosomes in the presence or absence of PY at 37°C programmed with a leaderless mRNA that was labeled on its 5' end with ³³P-labeled phosphate to follow binding, since leaderless mRNA does not bind to ribosomes in the absence of P-site tRNA (data not shown). Average values of three independent experiments with standard deviations are shown.

Schematic view of the experiment is shown underneath the columns: In the presence of PY, ribosomes were pre-incubated with the protein before the addition of the leaderless mRNA (starting with an AUG codon at the ribosomal P site at its 5' end) and the deacylated tRNA^{fMet}

B as in **A** but with an mRNA containing a Shine-Dalgarno sequence (which can bind to the ribosomes in the absence of tRNA) and deacylated tRNA^{fMet} that was labeled with ³³P-phosphate on its 5' end to follow binding. Experiments were carried out at 37°C or at 16°C. Average values of three independent experiments with standard deviations are shown.

Schematic view of the experiment is shown underneath the column: Protein Y was pre-incubated with the ribosome before the addition of the SD-mRNA (containing a Shine-Dalgarno sequence at its 5' end) and the deacylated tRNA^{fMet}.

A



B

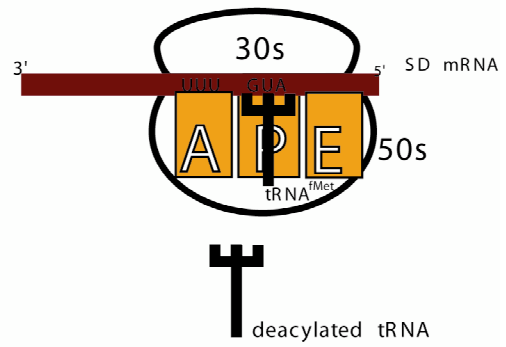
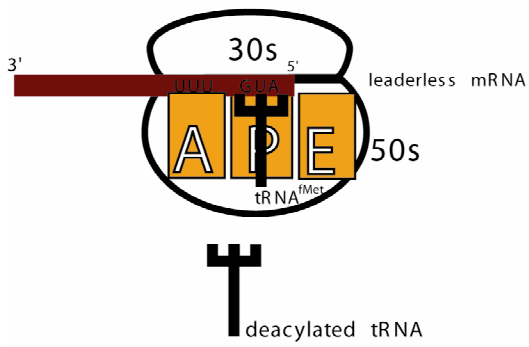
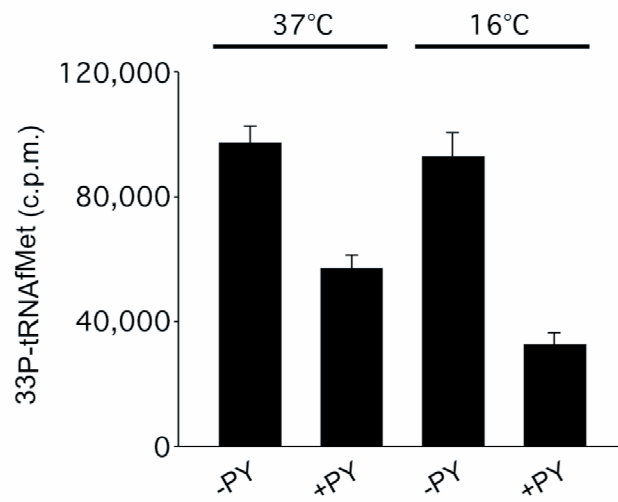


Figure 15: Inhibition of translation initiation by PY

A + B Experiments were performed using a buffer system that contained polyamines.

C + D Experiments were performed using a buffer system that contained no polyamines.

A Binding of ^{35}S -Methionine labeled fMet-tRNA^{fMet} to ribosomes at 37°C in the absence and presence of PY (-PY and +PY, respectively). Black, IFs were present in reactions (+IF); white, no IFs were present in the reactions (-IF). Average values of four independent experiments with standard deviations are shown.

B Reactions carried out as in **A** but at 16°C.

C Reactions carried out as in **A** but in the absence of polyamines.

D Reactions carried out as in **B** but in the absence of polyamines.

E Schematic view of the experiments: In the presence of PY, ribosomes were pre-incubated with the protein before the addition of mRNA, tRNA and IFs. Experiments were also done excluding this pre-incubation step revealing the same result.

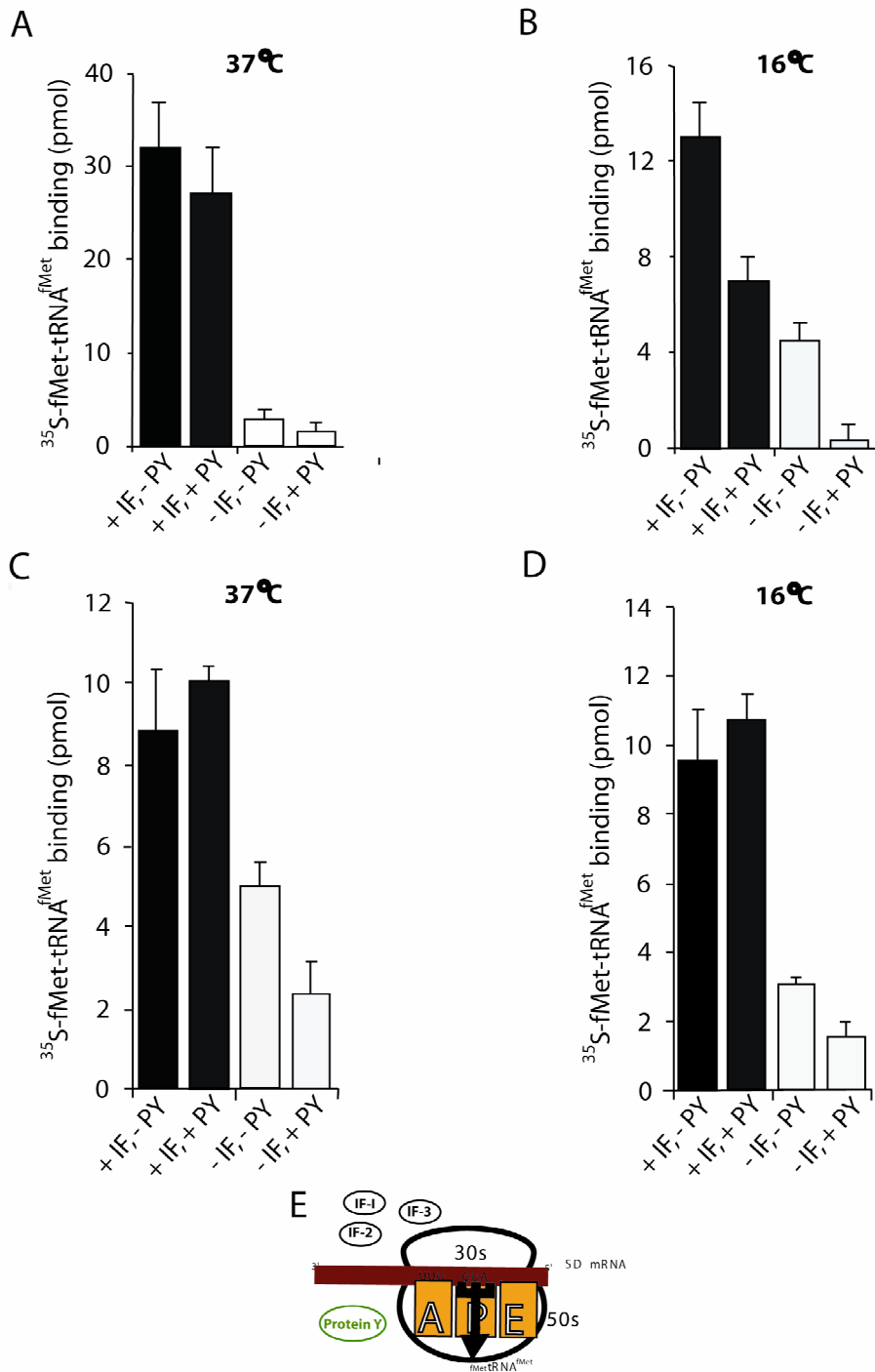


Figure 16: Ribosomal subunit association and dissociation.

A + B 1=70S, 2 = 70S +IF3, 3 = 70S + IF3 + IF1, 4 = 70S + PY, 5 = 70S + PY + IF3, 6 = 70S + PY + IF3 + IF1.

A Sucrose gradient profiles of 70S ribosomes in buffer containing polyamines. In gradients containing primarily 70S ribosomes, the small peak is from 50S subunit contamination of the 70S ribosome preparation.

B Sucrose gradients of 70S ribosomes in buffer without polyamines.

C Structural comparison of the binding site for IF1 with that for PY. IF1 is shown in red. The penultimate stem of 16S rRNA is shown in gold and the positive electron density for PY is shown in blue. Residues A1493 and C1400, marked with an asterisk, and the positions of the A and P sites are shown for reference.

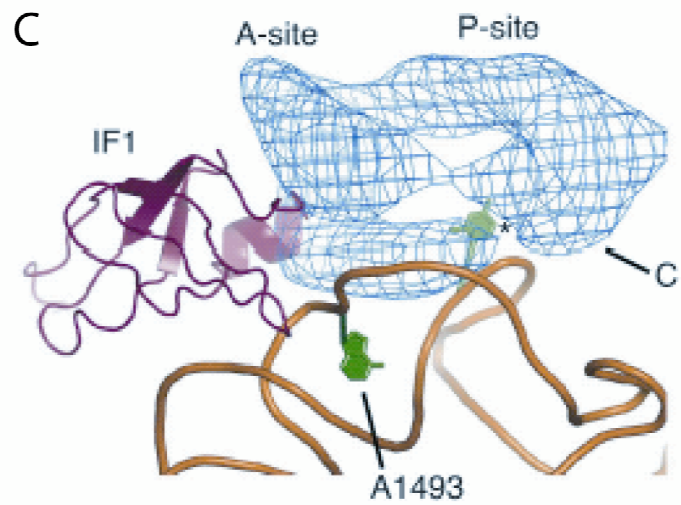
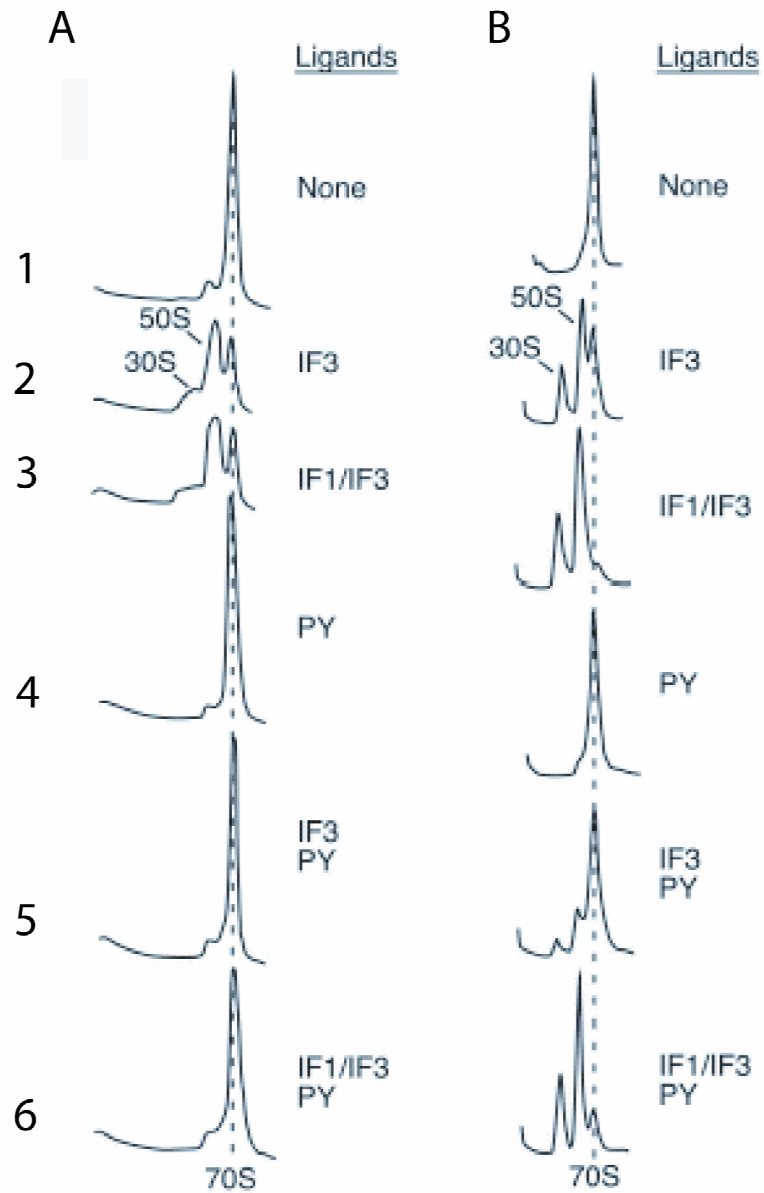


Figure 17: Inhibition of tRNA binding to the A site by PY

Binding of ^3H -labeled Phe-tRNA^{Phe} to the A site was tested in parallel to ^{35}S -labeled fMet tRNA^{fMet} binding to the P site in the presence and absence of Protein Y at **A** 16°C and **B** 37°C was tested. All experiments were done in a buffer system containing polyamines.

A + B 1: After the binding of ^{35}S labeled fMet tRNA^{fMet} to the ribosomal P site, PY was incubated with the complex before the addition of ^3H labeled Phe tRNA^{Phe} in complex with EF-Tu / GTP, 2: same as in 1 but without PY, 3: binding of ^{35}S labeled fMet tRNA^{fMet} to the ribosomal P site in the absence of PY and IFs, 4: ribosomes were pre-incubated with PY before the addition of ^{35}S labeled fMet tRNA^{fMet} to the ribosomal P site in the absence of IFs, 5: like 3 but in the presence of IFs, 6: like 4 but in the presence of IFs.

Average values of four independent experiments with standard deviations are shown.

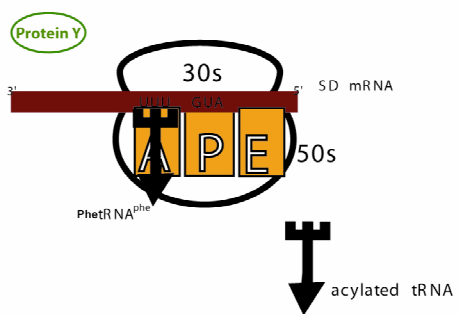
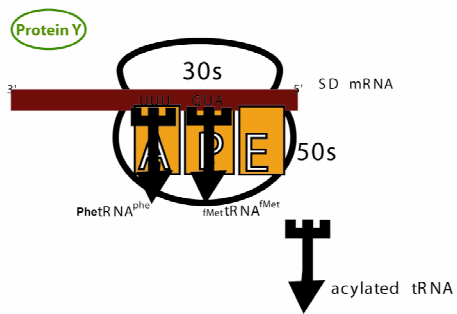
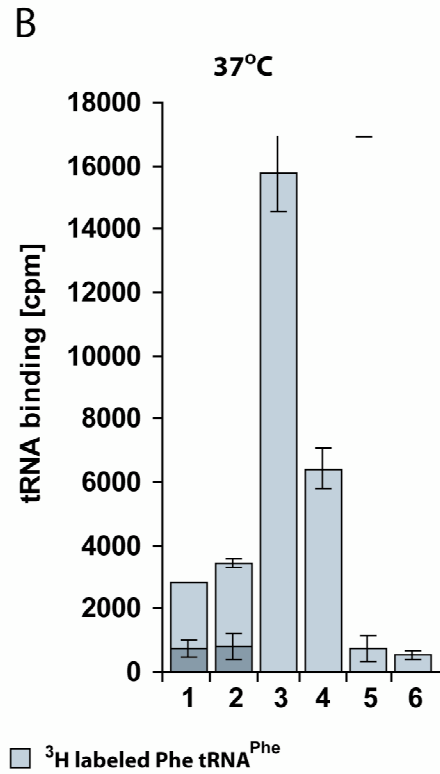
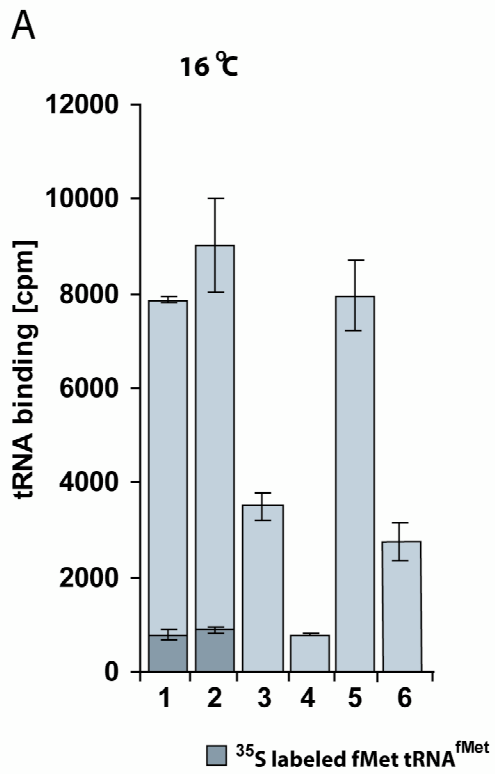


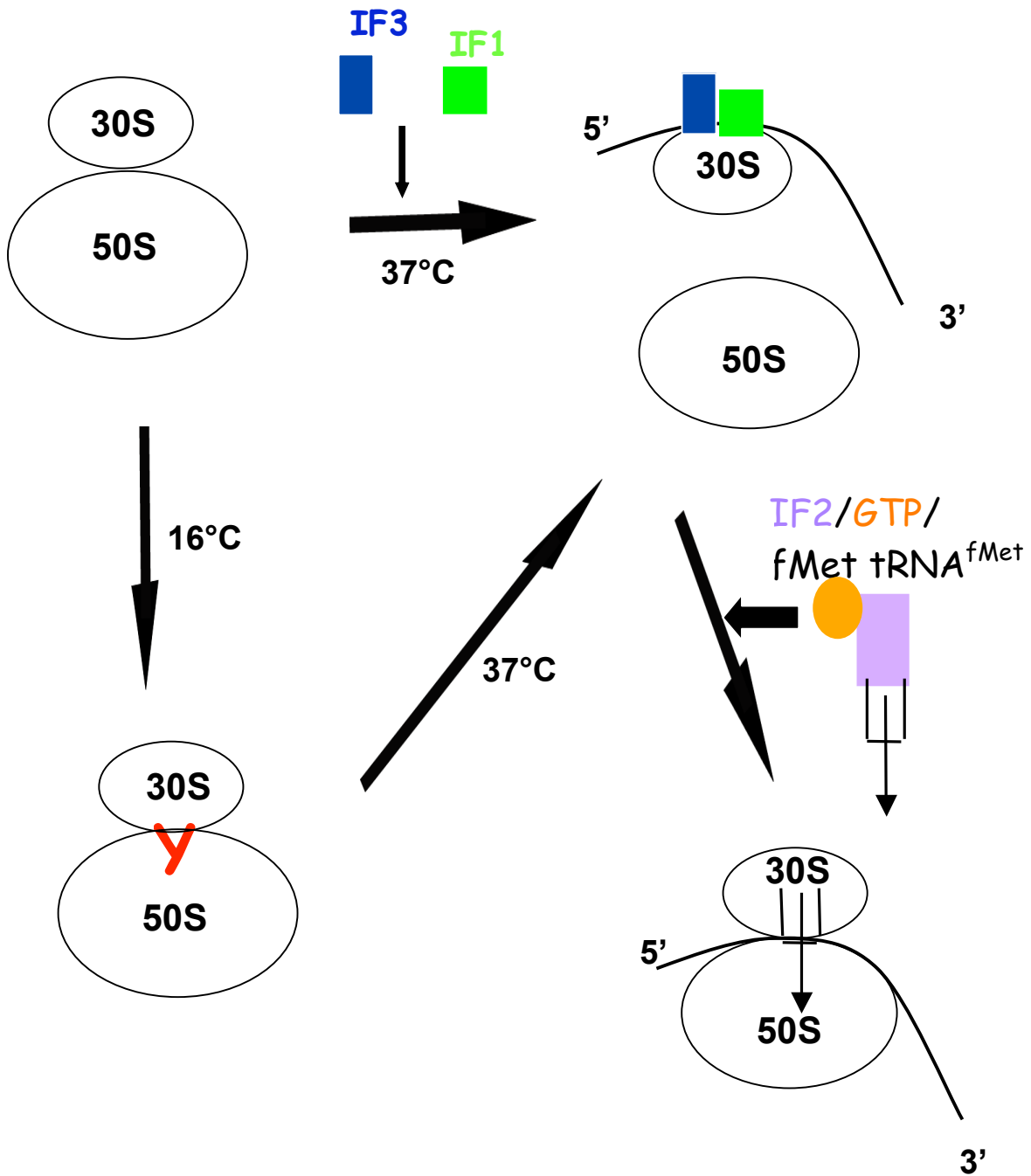
Figure 18: Control of translation initiation by Protein Y

This figure shows a scheme on how Protein Y may control translation during cold shock.

During normal growth conditions (37°C) IF1 and IF3 are working in concert to dissociate the two ribosomal subunits (upper left to upper right site) and bind to the 30S subunit. The initiator tRNA, fMet tRNA^{fMet} is then delivered to the ribosomal P site (lower right site). Upon subunit association the IFs are dissociating from the ribosome after which the ribosome will enter the elongation cycle (not shown).

Under cold shock conditions IF1 and IF3 are no longer able to dissociate the subunits and are replaced by Protein Y which stabilizes the 70S ribosome by binding to the P site (lower left site). Protein Y functions as a storage protein during cold shock until normal growth conditions reoccur and PY is replaced by IFs.

Protein Y is illustrated as a red Y.



Tables

Table 1: Diffraction statistics for the E.coli 70S ribosome crystals

	Apo 70S	70S-PY complex
Data collection		
Space group	I442	I442
Cell dimensions		
a, b, c (Å)	687.9, 687.9, 1933	685.8, 685.8, 1928.8
α, β, γ (°)	90, 90, 90	90, 90, 90
Resolution (Å)	500-11.35 (11.8-11.57)	500-10.98 (11.22-10.98)
R_{sym} or R_{merge} ^{a-c}	18.1 (46.2)	18.9 (47.7)
$I / \sigma I$ ^a	7.4 (2.0)	9.2 (2.1)
Completeness (%) ^a	93.9 (77.9)	94.2 (75.6)
Redundancy ^a	6.1 (2.6)	
Refinement ^d		
Resolution (Å)	500-11.5	
No.reflections, $R_{\text{work}}/R_{\text{free}}$ ^e	39.5/40.1	
No.atoms	714.210	

^a Values in parentheses are for the highest resolution shell. ^b For the apo 70S structure, three crystals were used for data measurement. For the 70S-PY complex, two crystals were used for data measurement. The mean crystal mosaicity for all crystals was 0.3°. ^c Three data measurement passes were used: a high-resolution sweep followed by two low-resolution sweeps. Thus the R_{merge} values in the low-resolution ranges and the overall R_{merge} value of the data are inflated. ^dRefinement involved rigid-body motions only. ^eAmplitudes with $\sigma > 0$.

Table 2: Concentrations of ions and polyamines important for ribosomal functions (Table is taken out of “The Ribosome: Structure, Function, Antibiotics and Cellular Interactions” (Nierhaus, Spahn et al. 2000))

System	Concn (mM)				
	Mg ²⁺	K ⁺ , NH ₄ ⁺ ^a	Polyamine		
			Spermidine	Spermine	Putrescine
Conventional buffer	7–20	100	None	None	None
Polyamine buffer	3–6	150	2	0.05	None ^b
In vivo ^c	~4	~150	1–4	~0.03	20 ^c

^a K⁺ and NH₄⁺ are more or less equivalent in in vitro systems of protein synthesis due to their similar ionic radii.

^b Putrescine has no effect on protein synthesis in vitro; additions of cadaverine and agmatine, which are also present in significant amounts in vivo, also have no effect on protein synthesis (Lewicki and Nierhaus, unpublished).

^c Lusk et al., 1968; Tabor and Tabor, 1985; Kamekura et al., 1987.